Irradiation-Induced Magnetism in Carbon Nanostructures

S. Talapatra,[1,2,*] P. G. Ganesan,[1] T. Kim,[1] R. Vajtai,[2] M. Huang,[3] M. Shima,[1] G. Ramanath,[1,2] D. Srivastava,[4] S. C. Deevi,[5] and P. M. Ajayan[1,2]

[1]*Department of MS & E, Rensselaer Polytechnic Institute, Troy, New York 12180-3590, USA*
[2]*Rensselaer Nanotechnology Center, Rensselaer Polytechnic Institute, Troy, New York 12180-3590, USA*
[3]*Department of Physics, SUNY Albany, New York 12203, USA*
[4]*NASA Ames Research Center, Moffett Field, California 94035, USA*
[5]*RD & E Center, Phillip Morris USA, Richmond, Virginia 23234, USA*

(Received 20 April 2005; published 23 August 2005)

Nitrogen (^{15}N) and carbon (^{12}C) ion implantations with implant energy of 100 keV for different doses were performed on nanosized diamond (ND) particles. Magnetic measurements on the doped ND show ferromagnetic hysteresis behavior at room temperature. The saturation magnetization (M_s) in the case of ^{15}N implanted samples was found to be higher compared to the ^{12}C implanted samples for dose sizes greater than 10^{14} cm^{-2}. The role of structural modification or defects along with the carbon-nitrogen (C-N) bonding states for the observed enhanced ferromagnetic ordering in ^{15}N doped samples is explained on the basis of x-ray photoelectron spectroscopy measurements.

DOI: 10.1103/PhysRevLett.95.097201 PACS numbers: 75.75.+a, 72.80.Ng, 75.50.Pp

Magnetism in carbon based systems has received a lot of attention recently. Developing magnetic systems with carbon has its own advantages. They are lightweight, stable, simple to process, and less expensive to produce. Investigations performed on various forms of carbon point towards the fact that it is possible to produce ferromagnetically interacting carbon systems [1–13]. It has been noted that the magnetic interactions in different forms of carbon can be ascribed to the electronic instabilities caused by bonding defects in these systems [1,2]. The presence of unpaired electron spins in a graphitic network can give rise to ferromagnetic behavior in them. Carbonaceous substances with a mixture of sp^2 and sp^3 coordinated atoms, nanographite, and fullerenes are known to show ferromagnetic behavior [1,2,11]. Recent reviews deal in greater detail with the aspects of proposed mechanisms of magnetism in various carbon based materials [1,2]. The possibility of introducing ferromagnetism by inducing a sp^3/sp^2 defect structure has been observed in a variety of carbon materials and is investigated for developing carbon based ferromagnetic materials. Different synthesis routes have been explored to fabricate magnetic carbons. Unconventional magnetism has been observed in nanostructured carbon foam produced by high power laser ablation of glassy carbon in argon atmosphere [3], which shows ferromagnetic behavior up to 90 K along with high saturation magnetization. Ferromagnetic spots and stable room temperature magnetic ordering in proton irradiated graphite was recently demonstrated [7]. The importance of hydrogen carbon bonding for ferromagnetic ordering was emphasized in this study. Subsequently, a spin polarized density functional theory calculation showed that vacancy-hydrogen complexes formed in proton irradiated graphite possess a magnetic moment that can lead to macroscopic magnetic signals [6].

Incorporation of certain trivalent impurities like nitrogen, phosphorous, and boron into carbon matrix also leads to ferromagnetism in carbon compounds [1]. Most of the previous studies on carbon-nitrogen systems were performed on organic substances produced by chemical processes [1,2] (and references therein). However, nitrogen can also be incorporated in carbon systems using physical methods. One of the most elegant ways to achieve incorporation of foreign species into solids is through ion implantation. Ion implantation has been routinely used as an efficient method for controlled doping of various carbon materials in the past (for example, bulk diamond to enhance electronic properties) [14,15]. The influence of ion implantation on the structure of various carbon based materials has also been investigated. In these studies, it has been shown that the process of ion implantation is capable of modifying the carbon structure by generating sp^2/sp^3 defects along with the incorporation of the implanted species in the carbon matrix. Similarly, defects and extended graphitic phases are also reported for ion implanted bulk diamonds [16]. In this Letter we report the effect of ^{15}N and ^{12}C implantation on the magnetic property and bonding modifications of nanosized diamond particles (ND). Evidence of room temperature ferromagneticlike behavior was obtained from the ion implanted nanodiamond particles that were absent for the unimplanted samples. Our results indicate that for lower doses the magnetic signals obtained for both the implants were similar. Beyond a critical dose size of 10^{14} cm^{-2}, the saturation magnetization for the ^{15}N doped samples was found to be relatively higher than the ^{12}C doped samples. A detailed investigation of the various C-N bonding states and structural modification of the ND under the influence of ^{15}N implants, using x-ray photoelectron spectroscopy (XPS), is also presented.

The nanodiamond samples used in this experiment were obtained from Ultradiamond Technologies Inc. (*Ultradiamond 90,* synthesized using a patented detonation process [17]). The reported average diameter of nanodiamond particles are within 4.0–5.0 nm. Thin uniform layers of the ND particles were deposited on cleaned silicon substrates. The ND particles were sonicated in acetone for 15 min prior to the deposition. Room temperature ion implantations for three different sets of samples were carried out. In the first set ^{15}N implant with dose sizes 5×10^{14}, 1×10^{15}, and $1 \times 10^{17}/\mathrm{cm}^2$ with implantation energy of 100 keV was performed. In the second set, keeping the implantation energy the same, we repeated the ^{15}N implant with dose sizes 1×10^{12}, 1×10^{13}, 1×10^{14}, 1×10^{15}, 1×10^{16}, and $5 \times 10^{16}/\mathrm{cm}^2$. In the third set ^{12}C ion implantation with dose sizes 1×10^{12}, 1×10^{13}, 1×10^{14}, 1×10^{15}, and $1 \times 10^{16}/\mathrm{cm}^2$ with implantation energy of 100 keV was performed.

Room temperature magnetization of the pristine and implanted samples was measured using a vibrating sample magnetometer (VSM; Lake Shore, Model No. VSM 7407). The magnetic data were obtained in an applied magnetic field between -0.4 to $+0.4$ T. For the first set of implants, the doped diamond particles were transferred to a thin film sample holder using scotch tape. The VSM measurements on the second and third sets of the implanted samples, however, were done by mounting the silicon piece ($\sim$10 mm $\times$ 10 mm) with the implanted diamond layer directly onto the sample holder. The samples were then mounted normal to the direction of the applied magnetic field. Deionizer was used to reduce the surface charge effects on the sample. To eliminate the possibility of any substrate contamination or spurious magnetic behavior, the measurements were also done on the original silicon substrate, silicon substrates doped with ^{15}N and ^{12}C, and the bare scotch tape used for lifting the implanted ND from the silicon substrate. These materials showed no signs of ferromagnetism. The various bonding configurations of the ^{15}N implanted samples from the first set were also analyzed using XPS. The XPS measurements were done on a PHI 5400 instrument with Mg $K\alpha$ probe beam under ultrahigh vacuum ($< 10^{-9}$ Torr) conditions.

The results of the VSM measurement on the ^{15}N implanted samples are presented in Fig. 1. In Fig. 1(a) a magnetic hysteresis curve of the doped diamond ND (with dose size $5 \times 10^{14}/\mathrm{cm}^2$ from the first set) measured at room temperature is shown. From the data it is clear that the doped ND developed a well defined ferromagnetic behavior, which was absent in the case of the pristine ND. Similar signals were obtained for all the implanted samples. Representative magnetization data from the second set of ^{15}N implants are shown in Fig. 1(b). Though at lower doses the increase in the magnetic saturation is not very pronounced, the data show evidence that all the implanted samples exhibit ferromagnetic behavior.

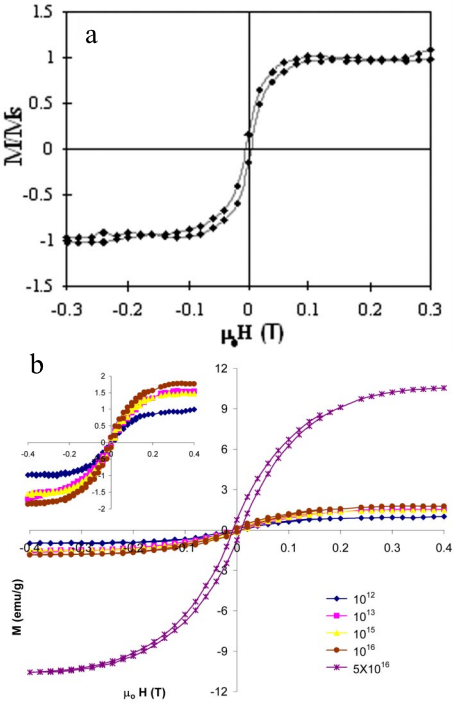

FIG. 1 (color online). (a) Magnetization as a function of the applied field for the sample with dose size $5 \times 10^{14}/\mathrm{cm}^2$ from the first set of implants. (b) Ferromagnetic signals from the ^{15}N implanted nanodiamonds for various doses from the second batch of samples presented.

The variation of the saturation magnetic moment (M_s) per unit mass with respect to the dose size for the ^{15}N implanted sample is presented in Fig. 2(a). The value of magnetization was within 0.9–11.5 emu/g for the whole doping range, comparable with other disorder carbon structure [1]. For calculating the saturation magnetic moment (M_s) per unit mass, an estimated ferromagnetically active volume of the irradiated samples, with a ^{15}N penetration depth of $\sim$80 nm was used.

The origin of magnetic signals from carbon based materials due to a mixture of sp^3 and sp^2 types of bonding has already been predicted in various previous studies [1,3,4,7,10]. To demonstrate the specific effect of nitrogen doping on the magnetic property of the nanodiamonds, a third set of implantation with ^{12}C using similar implantation parameters were carried out. This was performed because it is rational to expect that this set of ^{12}C implants will have defects generated comparable to the defects produced in the ^{15}N implantation. The magnetic moment contribution due to the disordered structure from these two species should be similar. Figure 2(b) shows the saturation magnetization values for the ^{12}C (calculated with a similar procedure as described for the case of ^{15}N implants) samples and ^{15}N irradiated samples. Note that the value of saturation magnetization for ^{15}N doped samples is comparatively higher than the ^{12}C implanted samples for dose sizes greater than 10^{14} cm^{-2}.

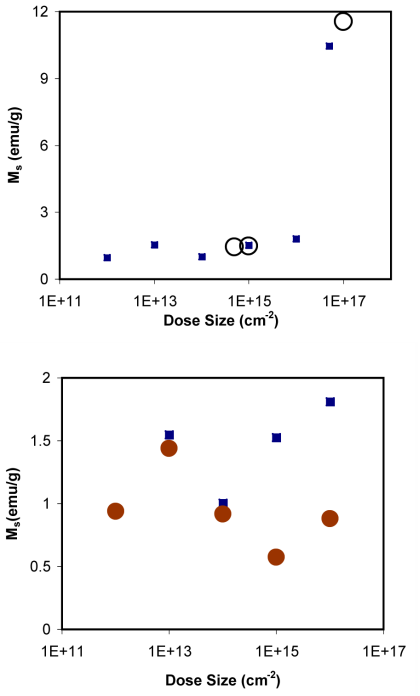

FIG. 2 (color online). Top: Saturation magnetic moment (open circles: first set of experiments; solid squares: second set of experiments) as a function of dose size for ^{15}N implants. Bottom: Comparison of the experimental values of saturation magnetic moments for ^{15}N (solid squares) and ^{12}C (solid circles) implants.

We have performed XPS studies on the implanted ND to investigate their structural modification due to the ^{15}N ion implantation. XPS has been extensively used to determine the bonding configuration of various carbon-nitrogen systems [18–22]. The XPS results on the pristine and ^{15}N implanted samples from the first set is presented in Fig. 3. The carbon 1s core level peak of the pristine nanodiamond is observed at 289.07 eV. This is about 3.47 eV greater than the solid-state tetrahedral bond configuration for carbon in diamond [18]. A corresponding N 1s spectrum shows a peak centered at 402.8 eV, indicating the presence of low level ($\sim$1.7 at. %) N impurities in the pristine sample [Fig. 3(e)]. Hence, the observed peak shift can be attributed to the combination of charging, C-N interactions, and surface oxidation. After ^{15}N implantation, the C 1s peak shifts to lower energy as a function of dopant concentration. In the $5 \times 10^{14}/cm^2$ and $1 \times 10^{15}/cm^2$ dose samples, the C 1s spectrum shows two subbands [Figs. 3(b) and 3(c)]. The lower energy band (285.5 eV) attributes to pure C-C sp^3 tetrahedral bonding, while the higher energy band ($\sim$287.5 eV) is assigned to C-N bonding in sp^3 hybridization [21,22]. The implant dose also influences the N content of the samples. It was observed that the ratio of (O-C-N)/(C-C) increases as the dose size is increased. The $5 \times 10^{14}/cm^2$ dosed sample exhibits 0.7 at. % of N, while the $10^{15}/cm^2$ dosed sample exhibit 1.2 at. % of N, and in the case of $10^{17}/cm^2$ dosed sample this value is 2.1%. The C 1s spectrum for $10^{17}/cm^2$ dose size shows three subbands [Fig. 3(d)]. The lowest energy band (284.5 eV) is assigned to sp^2 C-C bonds indicating change in the structure from diamond to graphite. The band centered at 286.5 eV is assigned to C-N in sp^2 hybridization. The higher energy band (289 eV) attributed to C═O bonds. The N 1s spectrum of implanted samples shows two subbands. The higher energy band ($\sim$401 eV) attributed to impurity nitrogen while the lower energy band ($\sim$399 eV) is attributed to the N implanted into the nanoparticles. The ratio of these two bands indicates that the implantation leads to annealing out of impurity N and incorporation of ^{15}N ion in the nanodiamond matrix.

A possible explanation for the difference in magnetization for the implanted samples could be as follows. For the low doses, the implantations result in defect generation in the nanodiamonds for both the implants, which is responsible for the magnetization. Above a certain dose of ^{15}N

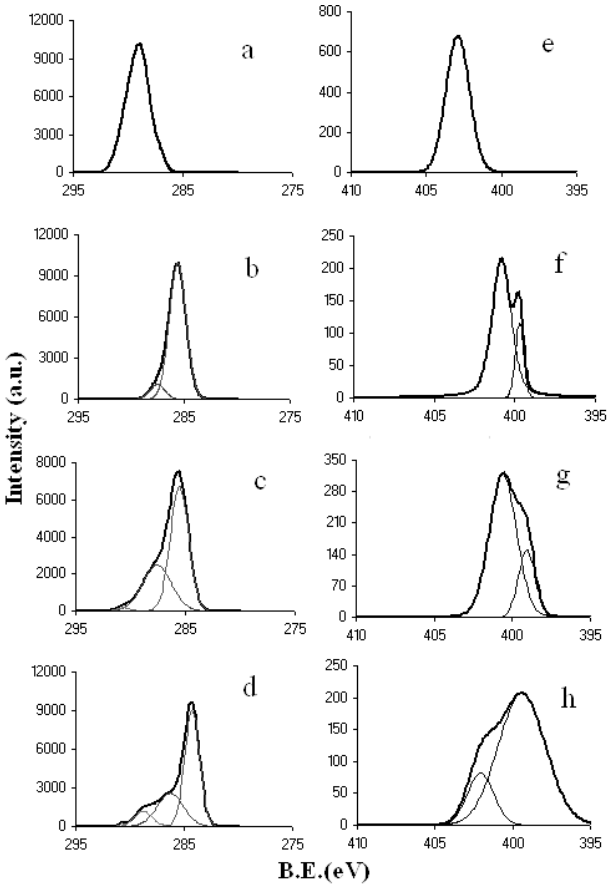

FIG. 3. XPS of the nanodiamond samples. (a)–(d) XPS spectra for carbon core level peaks. (a) Pristine nanodiamond. (b) Ion implanted ND with dose sizes $5 \times 10^{14}/cm^2$, (c) $1 \times 10^{15}/cm^2$, and (d) $1 \times 10^{17}/cm^2$. (e)–(h) XPS spectra showing nitrogen core level peaks. (e) Pristine nanodiamond. (f) Ion implanted ND with dose sizes $5 \times 10^{14}/cm^2$, (g) $1 \times 10^{15}/cm^2$, and (h) $1 \times 10^{17}/cm^2$.

extensive graphitization occurs in the sample and a significant amount of ^{15}N is trapped within the graphitic network. In our case the threshold dose for complete graphitization was found to be higher than 10^{15} cm^{-2} from the XPS analysis. Similar evidence of a minimum threshold dose needed for structural modification for the ND was also obtained from detailed transmission electron microscopy and Raman spectroscopy measurements [23]. For higher doses, extensive structural defects along with some incorporation of N atoms (evident from the formation of C-N bonding in different hybridization from the XPS data) into the extended graphitic phases can give rise to the presence of lone pair electron spin with the possibility of ferromagnetic ordering and an increased saturation magnetization. The ^{12}C implants were expected to produce structural changes in the ND similar to the ^{15}N. For higher doses ($> 10^{14}$ cm^{-2}) of ^{12}C implants, we speculate that annealing of defects or the broken C-C bonds (bond reconstruction between the implanted carbon and the carbon present in the nanodiamonds or graphitic phases) occurs during the implantation, thereby reducing the ferromagnetically active defect density in the ND structure. These results indicate that a reactive species, such as N or C (or H, Refs. [6,7]), which are capable of creating magnetic defect complexes or preventing recombination of interstitial-vacancy pairs, thereby stabilizing the magnetic state, is needed for inducing ferromagnetism in carbon structures. Note that implantation of He produces a negligible magnetic signal [7].

In conclusion, we have shown that ion irradiation of nanodiamond with ^{15}N and ^{12}C shows a signature of ferromagnetism. At low doses, the magnetization was independent of the doped species indicating that it mainly arises from structural deformation of the carbon bonds in nanodiamonds. ^{15}N implants exhibit a higher value of the saturation magnetization than ^{12}C implants at higher doses. This difference could be due to extensive defect generation or graphitization and, to some extent, incorporation of nitrogen in the graphitic network and formation of C-N bonds. The importance of the nature of the implanted species in inducing ferromagnetism in carbon structure is also demonstrated. Bonding modification of these nanodiamond particles under ^{15}N irradiation was also investigated and analyzed in this work. These results can lead to a better understanding of the ion implantation pathways into nanoparticles for encapsulation as well as magnetization and/or electronic nuclear spin applications in the high density memory or solid-state quantum bits areas, respectively. A quantification of the ferromagnetic contribution due to the doped N is complicated because of the formation of a variety of defects in the lattice, and will be investigated in the future.

The present work was supported by the Nanoscale Science and Engineering Initiative of the National Science Foundation under NSF Grant No. DMR-0117792 and Philip Morris USA. Part of this work was supported by NASA Ames JRI (NCC 2- 5494) and NASA Contract No. NAS2-03144. The authors sincerely thank Professor Saroj Nayak, Dr. Swastik Kar, Dr. Sujoy Roy, and Jake Ballard for helpful discussions.

*Electronic address: talaps@rpi.edu

[1] T. L. Makarova, in *Studies of High-Temperature Superconductivity* (NOVA Science Publishers, Inc., New York, 2003), p. 107.
[2] T. L. Makarova, Semiconductors **38**, 615 (2004).
[3] A. V. Rode, E. G. Gamaly, A. G. Christy, J. G. Fitzgerald, S. T. Hyde, R. G. Elliman, B. Luther-Davies, A. I. Veinger, J. Androulakis, and J. Giapintzakis, Phys. Rev. B **70**, 054407 (2004).
[4] K. Kusakabe and M. Maruyama, Phys. Rev. B **67**, 092406 (2003).
[5] P. O. Lehtinen, A. S. Foster, A. Ayuela, A. Krasheninnikov, K. Nordlund, and R. M. Nieminen, Phys. Rev. Lett. **91**, 017202 (2003).
[6] P. O. Lehtinen, A. S. Foster, Y. Ma, A. V. Krasheninnikov, and R. M. Nieminen, Phys. Rev. Lett. **93**, 187202 (2004).
[7] P. Esquinazi, D. Spemann, R. Hohne, A. Setzer, K.-H. Han, and T. Butz, Phys. Rev. Lett. **91**, 227201 (2003).
[8] K. Han, D. Spemann, P. Esquinazi, R. Hohne, V. Riede, and T. Butz, Adv. Mater. **15**, 1719 (2003).
[9] J. Jang and H. Yoon, Adv. Mater. **15**, 2088 (2003).
[10] Y. Shibayama, H. Sato, T. Enoki, and M. Endo, Phys. Rev. Lett. **84**, 1744 (2000).
[11] T. L. Makarova, B. Sundqvist, R. Hohne, P. Esquinazi, Y. Kopelevich, P. Scharff, V. A. Daydov, L. S. Kashevarova, and A. V. Rakhmanina, Nature (London) **413**, 716 (2001).
[12] S. Bandow, F. Kokai, K. Takahashi, M. Yudasaka, and S. Iijima, Appl. Phys. A **73**, 281 (2001).
[13] N. Park, M. Yoon, S. Berber, J. Ihm, E. Osawa, and D. Tomanek, Phys. Rev. Lett. **91**, 237204 (2003).
[14] J. F. Prins, Diam. Relat. Mater. **10**, 1756 (2001).
[15] R. Kalish, Carbon **37**, 781 (1999).
[16] C. Uzan-Saguy, C. Cytermann, R. Brener, V. Richter, M. Shaanan, and R. Kalish, Appl. Phys. Lett. **67**, 1194 (1995).
[17] http://www.ultradiamondtech.com/.
[18] F. L. Normand, J. Hommet, T. Szorenyi, C. Fuchs, and E. Fogarassy, Phys. Rev. B **64**, 235416 (2001).
[19] E. Maillard-Schaller, O. M. Kuettel, L. Diederich, L. Schlapbach, and V. V. Zhirnov, Diam. Relat. Mater. **8**, 805 (1999).
[20] C. Riccardi, R. Barni, E. Selli, G. Mazzone, M. R. Massafra, B. Marcandalli, and G. Poletti, Appl. Surf. Sci. **211**, 386 (2003).
[21] K. Yamamoto and H. Yoshida, Diam. Relat. Mater. **13**, 736 (2004).
[22] K. Yamamoto, T. Watanabe, K. Wazumi, and Y. Koga, Diam. Relat. Mater. **12**, 1061 (2003).
[23] S. Talapatra, J.-Y. Cheng, N. Chakrapani, A. Cao, R. Vajtai, M. B. Huang, S. Trasobares, and P. M. Ajayan (to be published).